

Electronic Supplementary Material (ESI) for Physical Chemistry Chemical Physics.

**Supplementary Information (SI) for
Prediction of ultraviolet optical materials in
the $K_2O-B_2O_3$ system**

Xiaoqing Guo, ‡ Yanting Wang, ‡ Haiyang Niu*

State Key Laboratory of Solidification Processing, International Center for Materials
Discovery, School of Materials Science and Engineering, Northwestern Polytechnical
University, Xi'an 710072, P.R. China

‡ These authors contributed equally to the work

*Corresponding Author: haiyang.niu@nwpu.edu.cn

Supplementary Discussion

Impact of temperature and pressure on phase stability.

As demonstrated by many precious studies, temperature has been found to play an important role in stabilizing structures that are metastable at 0 K. For instance, *oP112-1-KB₅O₈* is stable at 0 K ^[1], while *oP112-2-KB₅O₈* is a metastable phase at 0 K. Previous experimental research has shown that *oP112-2-KB₅O₈* can be synthesized at 760 °C, indicating its stability as a high-temperature phase ^[1]. Thus, for the newly predicted structures, particularly those that are metastable, synthesizing at elevated temperature presents a promising approach to realizing them in practice.

To clarify the impact of pressure on the stability of these structures, we have further calculated the thermodynamic convex hull at 3 GPa (Fig. S1). The metastable structures observed at 0 GPa, namely *mP28-2-K₃BO₃*, *mC72-KB₃O₅*, *oP112-2-KB₅O₈*, become thermodynamically stable at 3 GPa, suggesting that pressure enhances the stability of these structures. Notably, *mC72-KB₃O₅* has been successfully synthesized at 3 GPa and 600 °C in experiments and is recognized as a high-pressure phase in the literature ^[2-3], underscoring the reliability of our results. Therefore, considering the effects of temperature and pressure on phase stability, it is plausible that metastable phases in the K₂O-B₂O₃ system could be synthesized experimentally.

Nonlinear optical response.

The general expression for the nonlinear optical susceptibility depends on the frequency of $E(\omega)$. The second-order susceptibility tensor $\chi_{ijk}^{(2)}(-2\omega; \omega, \omega)$ is commonly represented as $\chi_{ijk}^{(2)}(\omega)$. Since that *hR21-K₃BO₃* belongs to the 3m point group, the non-zero components of the susceptibility tensor are: $\chi_{112}^{(2)}(\omega)$, $\chi_{131}^{(2)}(\omega)$, $\chi_{211}^{(2)}(\omega)$, $\chi_{222}^{(2)}(\omega)$, $\chi_{223}^{(2)}(\omega)$, $\chi_{311}^{(2)}(\omega)$, $\chi_{322}^{(2)}(\omega)$, and $\chi_{333}^{(2)}(\omega)$ (1, 2, and 3 refer to the *x*, *y* and *z* axes, respectively). Figs. S5a and S5b illustrate the real and imaginary parts of these eight second-order susceptibility components ^[4-5]. The trends of $\chi_{112}^{(2)}(\omega)$, $\chi_{311}^{(2)}(\omega)$, $\chi_{322}^{(2)}(\omega)$, and $\chi_{223}^{(2)}(\omega)$ are nearly coincident, while $\chi_{112}^{(2)}(\omega)$ and $\chi_{211}^{(2)}(\omega)$

exhibit identical trends. Therefore, we have analyzed the intraband and interband contributions to $\chi_{222}^{(2)}(\omega)$, $\chi_{333}^{(2)}(\omega)$, $\chi_{223}^{(2)}(\omega)$ and $\chi_{112}^{(2)}(\omega)$ (Figs. S5c-f). Among these, $\chi_{222}^{(2)}(\omega)$ and $\chi_{112}^{(2)}(\omega)$ have equal magnitudes but opposite signs, and they are the principal components of SHG.

Within the energy range of 0 to 2.3 eV, the real part changes slowly, and the imaginary part is zero, indicating that $\chi_{ijk}^{(2)}(\omega)$ is purely dispersive. Importantly, the 2ω terms dominate in the low energy regions, while high energy states exhibit mixed ω and 2ω terms. This distinction between ω and 2ω patterns highlights the relatively strong birefringence nature of *hR21-K₃BO₃*.

In addition, comparing the total contribution with the intraband and interband contributions, we find that the overall value of the second harmonic generation is very small due to the cancellation of intraband and interband components, which have values of opposite signs. Therefore, 2ω terms start contributing at an energy of $E_g/2$, while the ω terms begin contributing at energy above E_g . Consequently, any anisotropy in the linear optical properties is more significantly enhanced in the nonlinear spectra.

Supplementary Figures

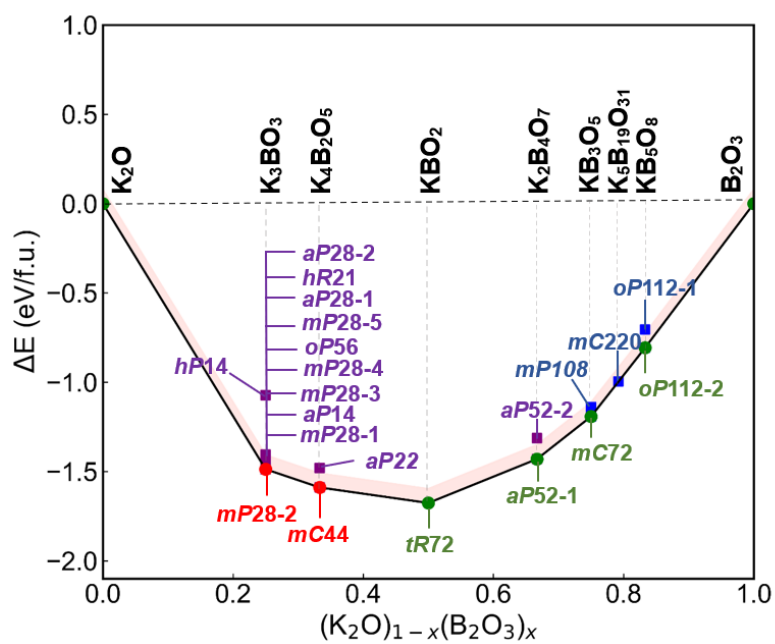
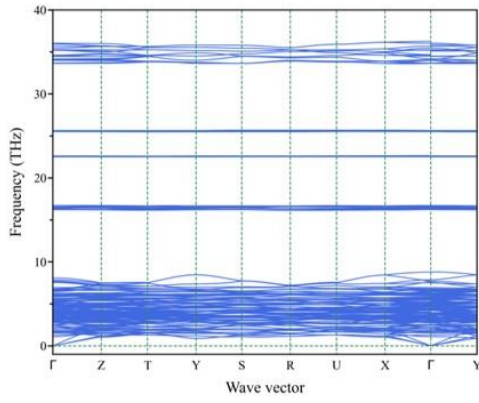
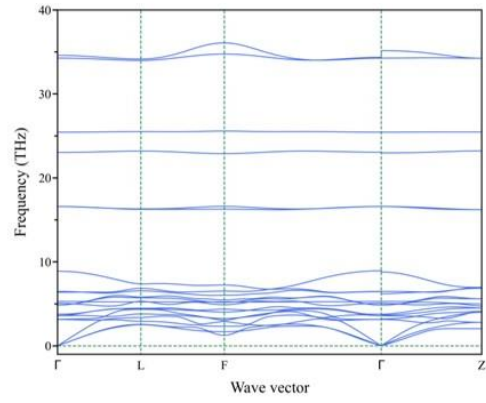


Figure S1. Thermodynamic convex hull of the K_2O - B_2O_3 system at 0 K and 3 GPa. Thermodynamically stable structures are denoted by red and green dots. Metastable structures are represented by purple and blue squares.

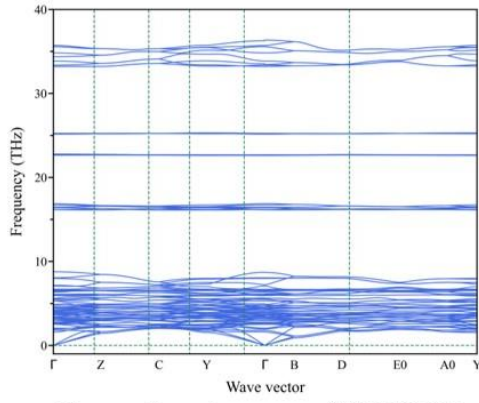
Phonon dispersion curves of *oP56*-K₃BO₃



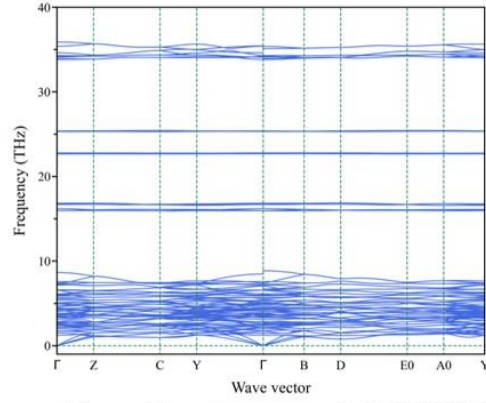
Phonon dispersion curves of *hR21*-K₃BO₃



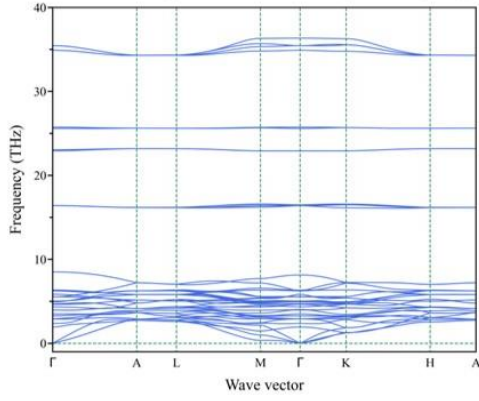
Phonon dispersion curves of *mP28-1*-K₃BO₃



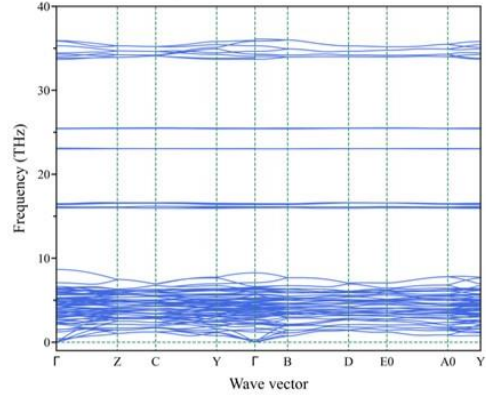
Phonon dispersion curves of *mP28-2*-K₃BO₃



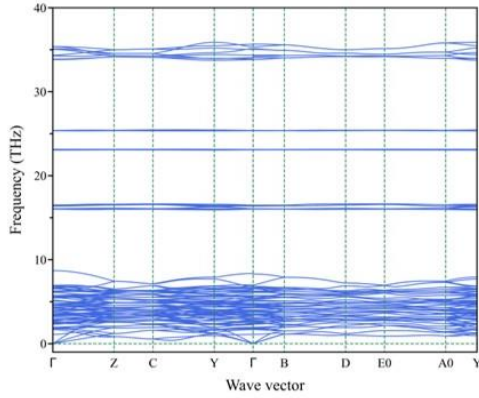
Phonon dispersion curves of *hP14*-K₃BO₃



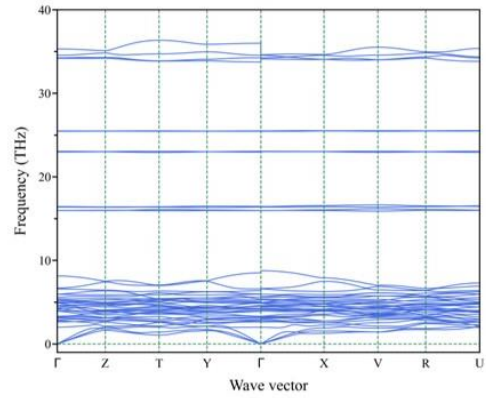
Phonon dispersion curves of *mP28-3*-K₃BO₃



Phonon dispersion curves of *mP28-4*-K₃BO₃



Phonon dispersion curves of *aP14*-K₃BO₃



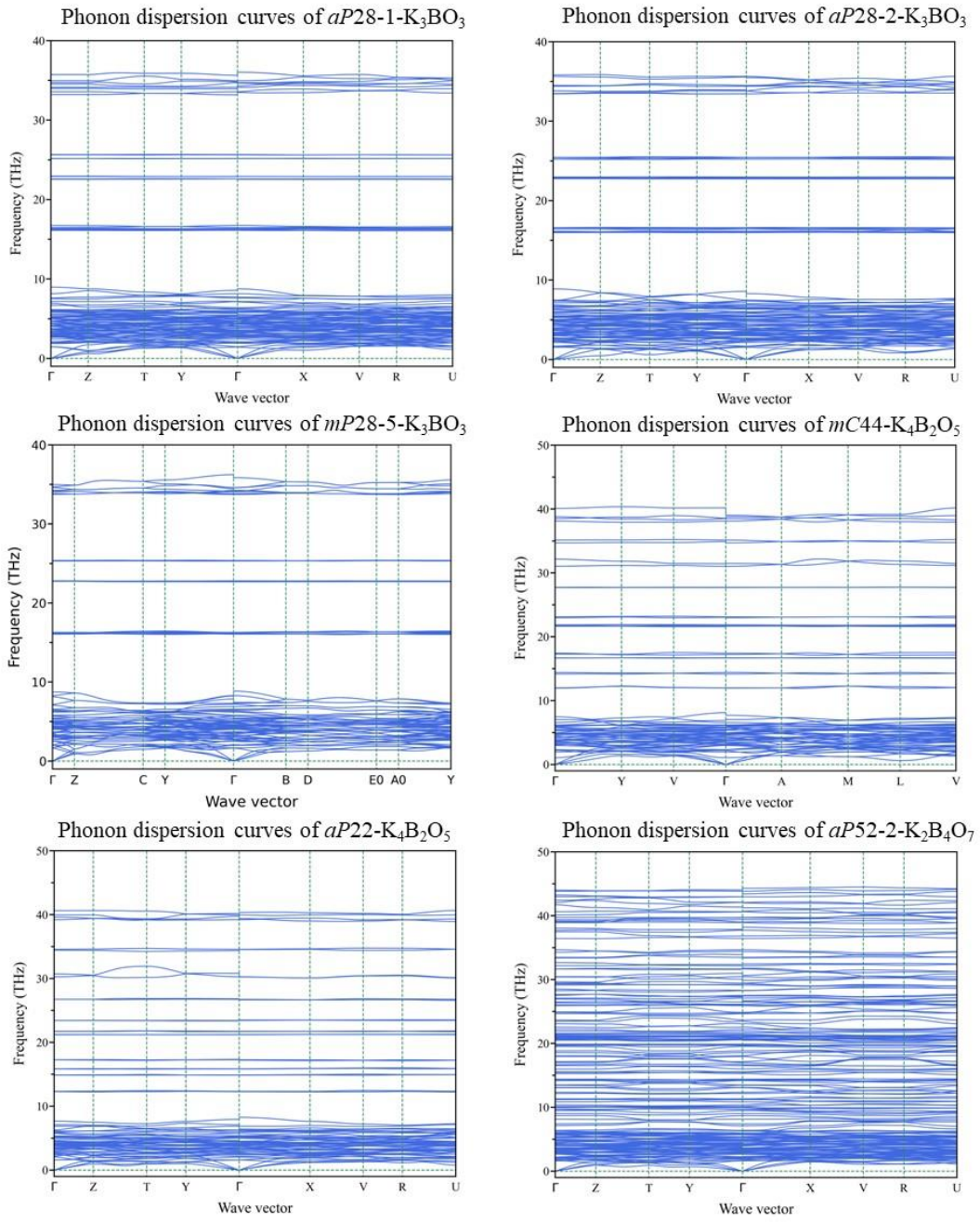


Figure S2. The phonon dispersion curves of fourteen predicted structures.

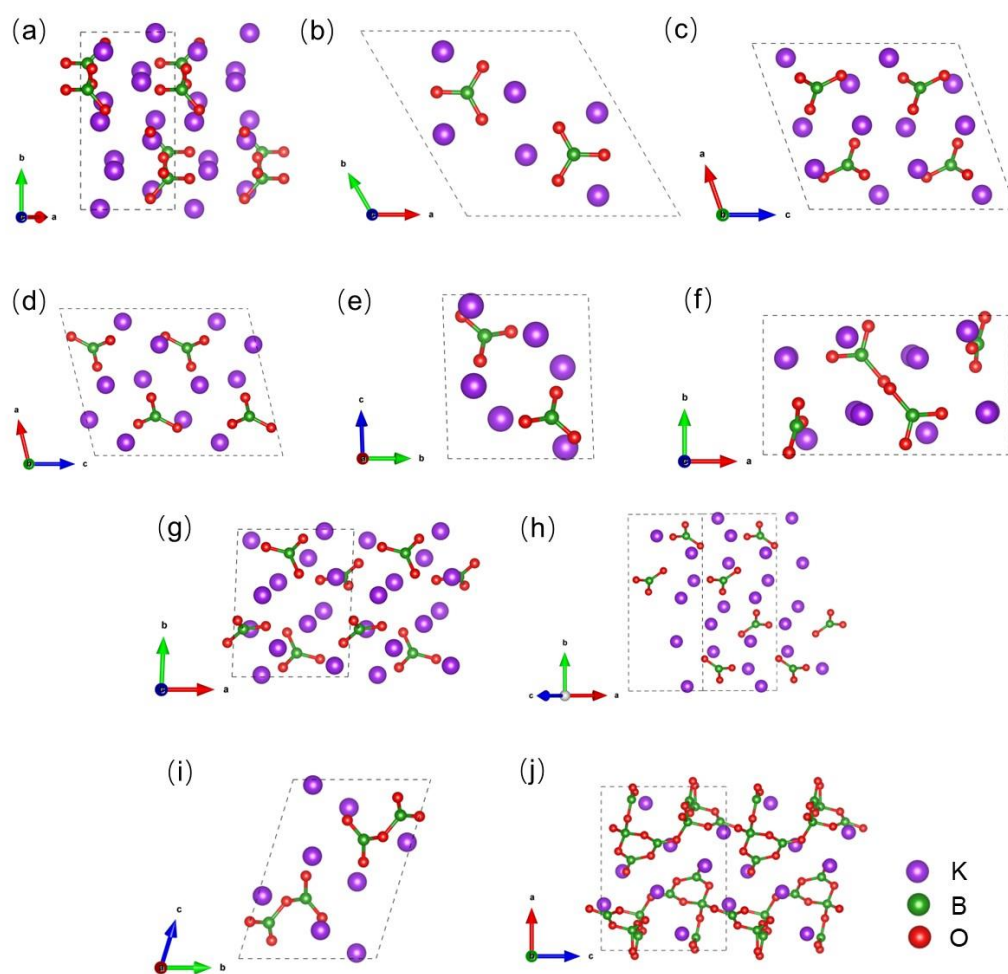
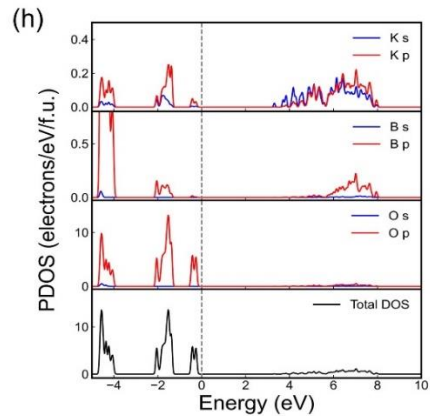
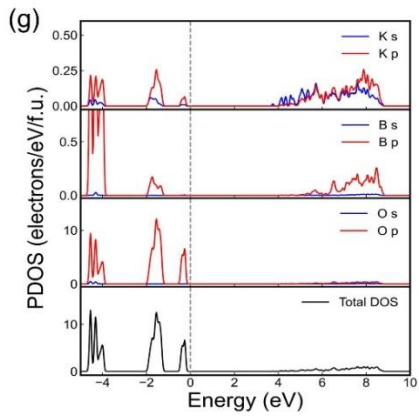
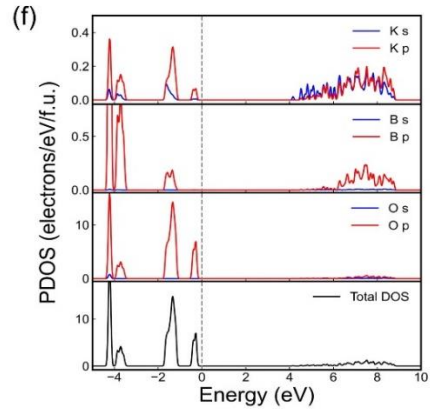
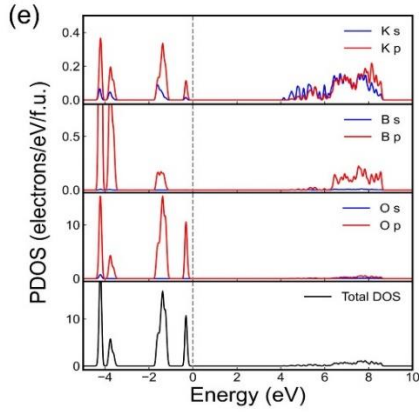
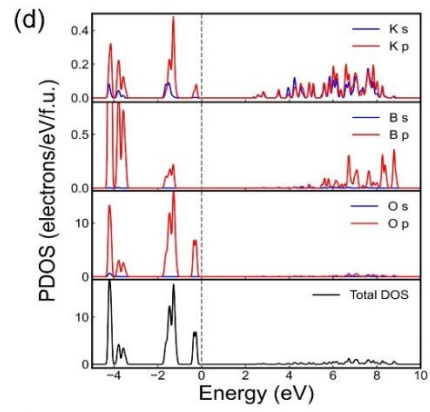
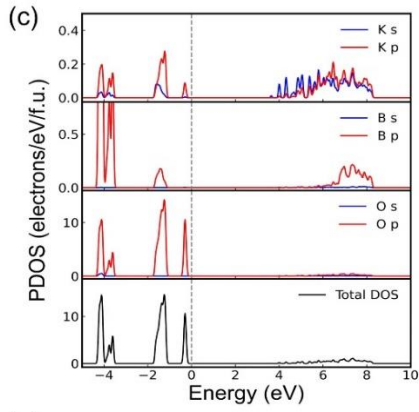
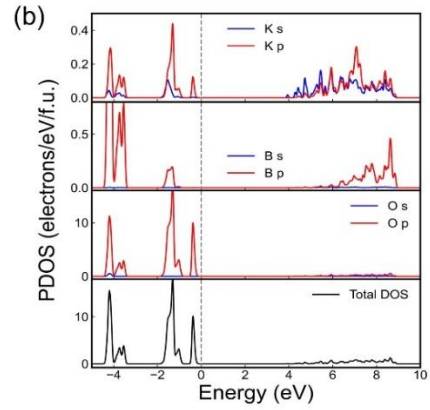
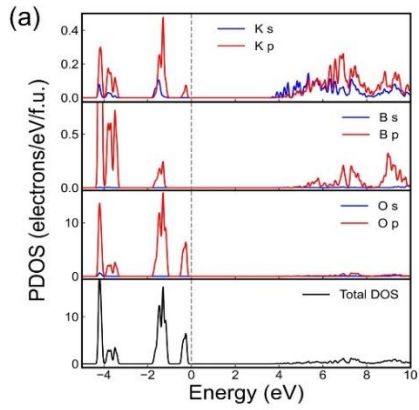


Figure S3. Crystal structures. (a) $mP28-2-K_3BO_3$, (b) $hP14-K_3BO_3$, (c) $mP28-3-K_3BO_3$, (d) $mP28-4-K_3BO_3$, (e) $aP14-K_3BO_3$, (f) $aP28-1-K_3BO_3$, (g) $aP28-2-K_3BO_3$, (h) $mP28-5-K_3BO_3$, (i) $aP22-K_4B_2O_5$, (j) $aP52-2-K_2B_4O_7$.



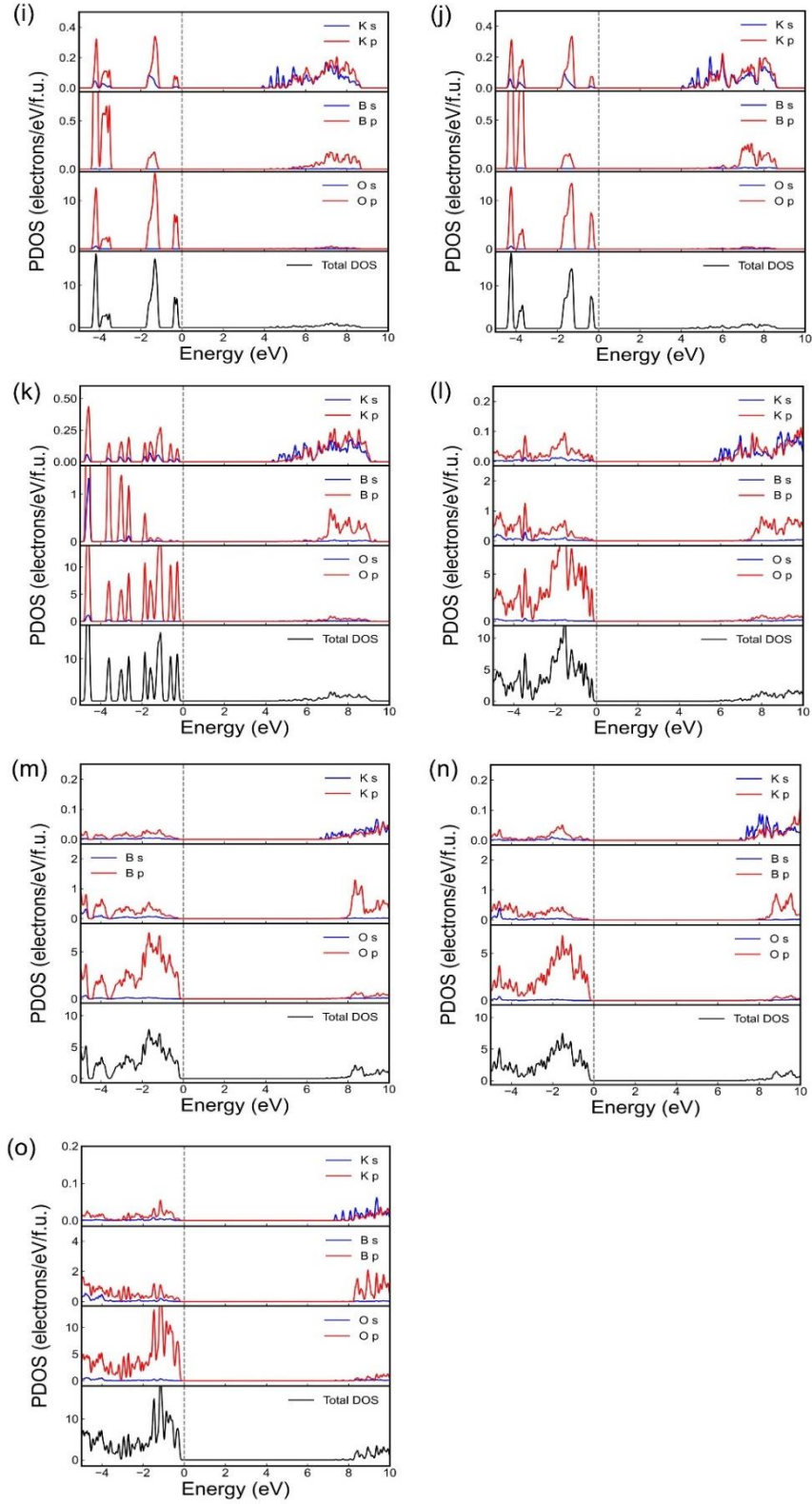


Figure S4. Projected density of states. (a) *hr21-K₃BO₃*, (b) *mP28-1-K₃BO₃*, (c) *mP28-2-K₃BO₃*, (d) *hP14-K₃BO₃*, (e) *mP28-3-K₃BO₃*, (f) *mP28-4-K₃BO₃*, (g) *aP14-K₃BO₃*, (h) *aP28-1-K₃BO₃*, (i) *aP28-2-K₃BO₃*, (j) *mP28-5-K₃BO₃*, (k) *aP22-K₄B₂O₅*, (l) *aP52-2-K₂B₄O₇*, (m) *mP108-KB₃O₅*, (n) *mC72-KB₃O₅*, (o) *oP112-2-KB₅O₈*.

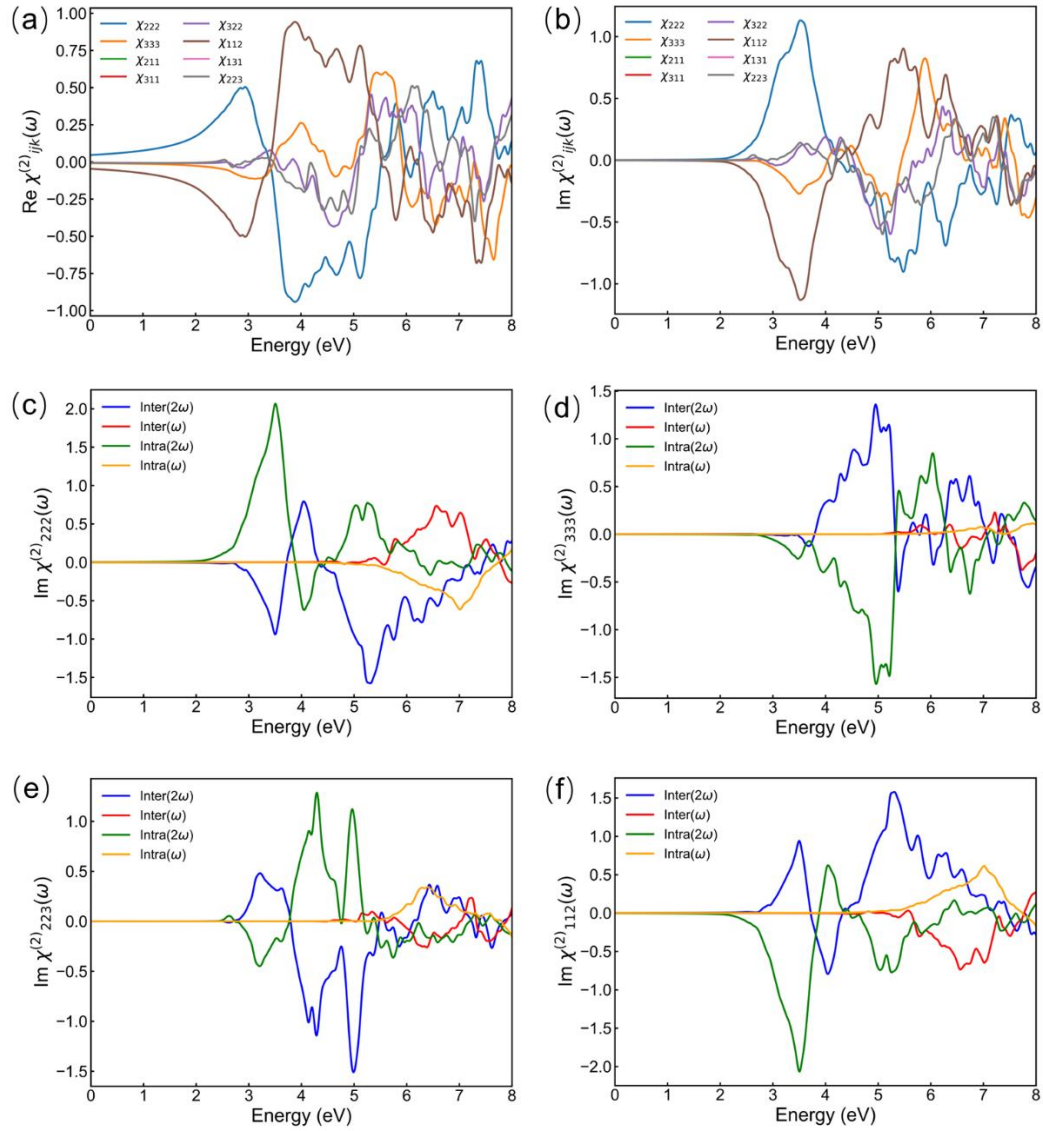


Figure S5. Calculated (a) real and (b) imaginary parts of $\chi_{ijk}^{(2)}(\omega)$. Calculated (c) $\text{Im } \chi_{222}^{(2)}(\omega)$, (d) $\text{Im } \chi_{333}^{(2)}(\omega)$, (e) $\text{Im } \chi_{223}^{(2)}(\omega)$, (f) $\text{Im } \chi_{112}^{(2)}(\omega)$ spectra along with the intraband and interband contributions. All $\text{Im } \chi_{ijk}^{(2)}(\omega)$ are given in units of 10^{-7} esu.

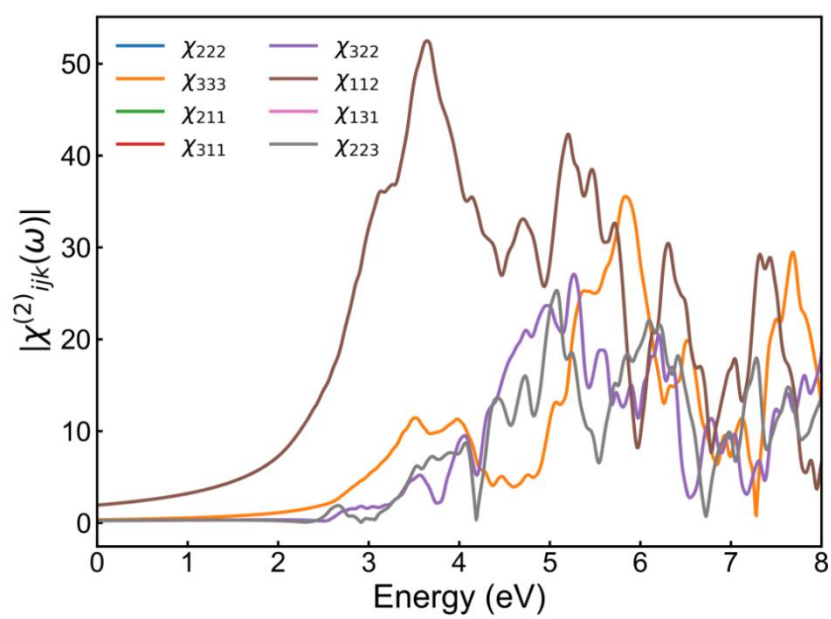


Figure S6. Calculated absolute values of $\chi_{ijk}^{(2)}(\omega)$. All $|\chi_{ijk}^{(2)}(\omega)|$ are expressed in units of pm/V.

Supplementary Tables

Table S1. Crystal structural information and bond valence sum (BVS) for predicted structures.

Phase	Pearson symbol	Space group & cell (Å)	Atom	Wyckoff position	x(a)	y(b)	z(c)	ΔE (eV/f.u.)	BVS
K₃BO₃	<i>oP56</i>	<i>Pbam</i> a=10.1355, b=10.2473, c=9.6536, $\alpha=\beta=\gamma=90^\circ$	K1	<i>8i</i>	0.2530	0.2628	0.2498	-1.4804	0.864
			K2	<i>4g</i>	0.3432	0.4816	0.0000		0.998
			K3	<i>4h</i>	0.4792	0.1619	0.5000		0.974
			K4	<i>4f</i>	0.5000	0.0000	0.1849		1.006
			K5	<i>4e</i>	0.5000	0.5000	0.3157		1.060
			B1	<i>4h</i>	0.2483	0.4660	0.5000		2.733
			B2	<i>4g</i>	0.4558	0.7486	0.0000		2.736
			O1	<i>8i</i>	0.3037	0.0101	0.3730		1.774
			O2	<i>4h</i>	0.3491	0.3727	0.5000		2.013
K₃BO₃	<i>hR21</i>	<i>R3m</i> a=b=10.7671, c=3.935, $\alpha=\beta=90^\circ, \gamma=120^\circ$	K1	<i>9b</i>	0.8799	0.1201	0.5327	-1.4800	0.945
			B1	<i>3a</i>	0.0000	0.0000	0.0364		2.733
			O1	<i>9b</i>	0.0754	0.1507	0.0373		1.856
K₃BO₃	<i>mP28-1</i>	<i>P2₁/c</i> a=6.1891, b=7.0517, c=12.2249, $\alpha=\gamma=90^\circ$, $\beta=111.69^\circ$	K1	<i>4e</i>	0.2996	0.4982	0.1082	-1.4768	1.021
			K2	<i>4e</i>	0.2970	0.4989	0.5914		0.947
			K3	<i>4e</i>	0.1372	0.6643	0.8177		0.902
			B1	<i>4e</i>	0.2909	0.2333	0.3945		2.718
			O1	<i>4e</i>	0.5070	0.7536	0.5048		2.057
			O2	<i>4e</i>	0.0716	0.2254	0.4055		1.765
			O3	<i>4e</i>	0.3063	0.2799	0.7823		1.762
K₃BO₃	<i>mP28-2</i>	<i>P2₁/c</i> a=6.3963, b=9.1951, c=10.3901, $\alpha=\gamma=90^\circ$, $\beta=127.28^\circ$	K1	<i>4e</i>	0.8607	0.1090	0.5600	-1.4592	0.744
			K2	<i>4e</i>	0.7995	0.5047	0.5470		1.016
			K3	<i>4e</i>	0.4518	0.7801	0.2984		1.026
			B1	<i>4e</i>	0.2638	0.3235	0.8446		2.726
			O1	<i>4e</i>	0.6990	0.5621	0.2293		1.785
			O2	<i>4e</i>	0.4415	0.2063	0.9105		2.060
			O3	<i>4e</i>	0.9447	0.8254	0.6441		1.667
K₃BO₃	<i>hP14</i>	<i>P6₃/m</i> a=b=9.8507, c=4.0335, $\alpha=\beta=90^\circ, \gamma=120^\circ$	K1	<i>6h</i>	0.6696	0.1110	0.7500	-1.4464	0.939
			B1	<i>2d</i>	0.3333	0.6667	0.7500		2.748
			O1	<i>6h</i>	0.3304	0.5227	0.7500		1.855
K₃BO₃	<i>mP28-3</i>	<i>P2₁/c</i> a=9.0306, b=5.3518, c=10.5727, $\alpha=\gamma=90^\circ$, $\beta=109.03^\circ$	K1	<i>4e</i>	0.4939	0.7925	0.6044	-1.4449	0.996
			K2	<i>4e</i>	0.7565	0.8874	0.9068		0.796
			K3	<i>4e</i>	0.0875	0.5506	0.8608		0.794
			B1	<i>4e</i>	0.2673	0.9140	0.7595		2.731
			O1	<i>4e</i>	0.3977	0.7692	0.8296		1.751
			O2	<i>4e</i>	0.1942	0.8773	0.6214		1.891
K₃BO₃		<i>P2₁/c</i> a=8.6535, b=5.3321,	K1	<i>4e</i>	0.2555	0.6200	0.4845		0.831
			K2	<i>4e</i>	0.0194	0.2749	0.8524		0.949
			K3	<i>4e</i>	0.4111	0.4697	0.8188		0.924

K₃BO₃	<i>mP28-4</i>	c=10.7458, α=90°, β=103.47°, γ=90°	B1	4e	0.2330	0.1194	0.6277	-1.4381	2.729
			O1	4e	0.2847	0.9494	0.7293		1.703
			O2	4e	0.1052	0.2826	0.6259		1.676
			O3	4e	0.3102	0.3757	0.0263		1.941
K₃BO₃	<i>aP14</i>	a=5.4682, b=6.3878, c=7.1551, α=99.06°, β=99.27°, γ=101.20°	K1	2i	0.2960	0.3695	0.2434		0.818
			K2	2i	0.2415	0.8082	0.0680		1.004
			K3	2i	0.2104	0.8074	0.5565		0.910
			B1	2i	0.2467	0.2801	0.7486	-1.4320	2.731
			O1	2i	0.7768	0.8719	0.1295		1.646
			O2	2i	0.1370	0.4615	0.7742		1.757
			O3	2i	0.3791	0.2469	0.5972		1.807
K₃BO₃	<i>aP28-1</i>	a=6.3446, b=7.2240, c=11.2510, α=94.22°, β=104.94°, γ=93.75°	K1	2i	0.6977	0.9459	0.9035		1.051
			K2	2i	0.6935	0.4846	0.3767		1.082
			K3	2i	0.7106	0.9919	0.3983		0.869
			K4	2i	0.6921	0.4491	0.9098		0.791
			K5	2i	0.8874	0.2013	0.1743		0.925
			K6	2i	0.8426	0.3391	0.6609		0.770
			B1	2i	0.7172	0.7313	0.6033		2.712
			B2	2i	0.2056	0.2617	0.8651	-1.4239	2.737
			O1	2i	0.4746	0.2466	0.4877		2.014
			O2	2i	0.7039	0.6850	0.7207		1.960
			O3	2i	0.0142	0.1957	0.8955		1.673
			O4	2i	0.3669	0.1403	0.8577		1.778
			O5	2i	0.9224	0.7746	0.5751		1.649
			O6	2i	0.2349	0.4491	0.8431		2.023
K₃BO₃	<i>aP28-2</i>	a=6.7031, b=8.5088, c=8.8861, α=87.80°, β=88.11°, γ=87.64°	K1	2i	0.6344	0.3588	0.4291		0.762
			K2	2i	0.8804	0.0757	0.8432		0.825
			K3	2i	0.7664	0.4468	0.0154		0.982
			K4	2i	0.7468	0.9873	0.4633		1.051
			K5	2i	0.8612	0.6765	0.6976		0.904
			K6	2i	0.6156	0.8049	0.1546		0.940
			B1	2i	0.5490	0.1612	0.1744		2.720
			B2	2i	0.9194	0.6771	0.3548	-1.4206	2.723
			O1	2i	0.5404	0.6992	0.8863		1.925
			O2	2i	0.4354	0.0639	0.2719		1.881
			O3	2i	0.9719	0.6187	0.2127		1.764
			O4	2i	0.9483	0.2305	0.5704		1.915
			O5	2i	0.7521	0.1204	0.1423		1.503
			O6	2i	0.7261	0.6565	0.4178		1.919
K₃BO₃	<i>mP28-5</i>	a=5.5350, b=14.3019, c=7.2498, α=γ=90°, β=124.27°	K1	4e	0.4953	0.2791	0.8542		0.999
			K2	4e	0.5766	0.9751	0.2887		0.966
			K3	4e	0.9456	0.8768	0.1147		0.745
			B1	4e	0.0504	0.8760	0.7172	-1.4142	2.720
			O1	4e	0.3470	0.6290	0.3949		1.913
			O2	4e	0.0620	0.3198	0.9741		1.667
			O3	4e	0.8654	0.5603	0.2283		1.850
K₄B₂O₅	<i>mC44</i>	a=11.7267, b=9.1359, c=6.9802, α=γ=90°	K1	8f	0.8595	0.5397	0.0770		0.967
			K2	8f	0.8611	0.8364	0.7341		0.891
			B1	8f	0.0874	0.1790	0.6728	-1.5636	2.772
			O1	8f	0.0521	0.6985	0.0528		1.833

		$\beta=109.38^\circ$	O2	4e	0.0000	0.8913	0.2500		1.804
			O3	8f	0.6993	0.3849	0.2191		1.895
K₄B₂O₅	aP22	$\bar{P1}$ a=5.5174, b=7.5099, c=10.3114, $\alpha=70.62^\circ$, $\beta=75.21^\circ$, $\gamma=77.19^\circ$	K1	2i	0.2945	0.9668	0.1496		0.951
			K2	2i	0.7144	0.1546	0.4692		1.042
			K3	2i	0.7410	0.3082	0.0718		0.886
			K4	2i	0.1831	0.4673	0.3430		0.814
			B1	2i	0.7419	0.6458	0.1642		2.773
			B2	2i	0.8006	0.8599	0.3000	-1.5087	2.767
			O1	2i	0.4043	0.9997	0.7060		1.940
			O2	2i	0.2939	0.5163	0.7276		1.765
			O3	2i	0.1161	0.2209	0.8196		1.885
			O4	2i	0.0508	0.2001	0.6002		1.845
			O5	2i	0.3367	0.3064	0.9611		1.666
K₂B₄O₇	aP52	$\bar{P1}$ a=6.9441, b=8.8709, c=11.6204, $\alpha=94.71^\circ$, $\beta=94.87^\circ$, $\gamma=92.33^\circ$	K1	2i	0.6343	0.0524	0.1429		1.038
			K2	2i	0.4913	0.5214	0.7793		0.992
			K3	2i	0.8316	0.6704	0.9827		0.912
			K4	2i	0.8582	0.8544	0.3985		1.154
			B1	2i	0.6782	0.2578	0.5784		2.924
			B2	2i	0.5651	0.7957	0.5870		2.930
			B3	2i	0.9739	0.4517	0.2854		2.929
			B4	2i	0.8436	0.0502	0.8447		2.921
			B5	2i	0.8739	0.3071	0.7839		3.135
			B6	2i	0.7891	0.2534	0.3773		2.944
			B7	2i	0.9012	0.8084	0.7158		2.912
			B8	2i	0.6784	0.2622	0.9484		2.847
			O1	2i	0.9068	0.1479	0.3156	-1.4211	1.948
			O2	2i	0.8223	0.2487	0.5058		1.977
			O3	2i	0.1761	0.5898	0.6526		1.996
			O4	2i	0.4225	0.7890	0.6613		2.051
			O5	2i	0.2956	0.7104	0.3040		1.934
			O6	2i	0.0429	0.8448	0.2030		1.977
O7	2i	0.2032	0.6364	0.1048		2.035			
O8	2i	0.0320	0.4048	0.7540		1.862			
O9	2i	0.4842	0.2327	0.5335		2.039			
O10	2i	0.2891	0.8972	0.0779		2.101			
O11	2i	0.4532	0.7000	0.9800		1.753			
O12	2i	0.8854	0.6463	0.7441		1.931			
O13	2i	0.7555	0.8318	0.6182		1.951			
O14	2i	0.8536	0.8976	0.8250		1.868			

References

- 1 Krogh-Moe J. The crystal structure of the high-temperature modification of potassium pentaborate[J]. Acta Crystallographica Section B: Structural Crystallography and Crystal Chemistry, 1972, 28(1): 168-172.
- 2 Bubnova R S, Fundamenskii V S, Filatov S K, et al. Crystal structure and thermal behavior of KB_3O_5 [C]. Doklady Physical Chemistry. New York: Consultants Bureau., 2004, 398(4-6): 249-253.
- 3 Neumair S C, Vanicek S, Kaindl R, et al. HP- KB_3O_5 Highlights the Structural Diversity of Borates: Corner-Sharing BO_3/BO_4 Groups in Combination with Edge-Sharing BO_4 Tetrahedra[J]. 2011.
- 4 Rashkeev S N, Lambrecht W R L, Segall B. Efficient ab initio method for the calculation of frequency-dependent second-order optical response in semiconductors[J]. Physical Review B, 1998, 57(7): 3905.
- 5 Hu C L, Xu X, Sun C F, et al. Electronic structures and optical properties of $\text{Ca}_5(\text{BO}_3)_3\text{F}$: a systematical first-principles study[J]. Journal of Physics: Condensed Matter, 2011, 23(39): 395501.